Theoretical and Applied Climatology (2019) 138:433–447
https://doi.org/10.1007/s00704-019-02824-w

ORIGINAL PAPER

Spatial and temporal variation of the near-surface wind regimes in the Taklimakan Desert, Northwest China

Zhengyao Liu[1] · Zhibao Dong[1] · Zhengcai Zhang[2] · Xujia Cui[1] · Nan Xiao[1]

Received: 22 March 2018 / Accepted: 25 February 2019 / Published online: 19 March 2019

Abstract

The characteristics of eolian sand activity are greatly influenced by the wind regime, and wind regimes have been changing around the world in response to climate change. This has also been true in the desert area of northwestern China since 1965, and these changes have changed the region's landforms, sandstorm frequency, and desertification. In this study, we analyzed the temporal and spatial variation of the region's near-surface wind field since 1965. We found an average annual wind speed during this period of 1.7 m s^{-1}, with a decreasing trend from 1965 to 2000 and an increasing trend from 2000 to 2015. The maximum rate of decrease occurred in the spring and in the eastern Taklimakan Desert. The variation of the average wind speed depended on the frequency of winds strong enough to entrain sand (with a wind speed > 6 m s^{-1}). We also found that variations of the drift potential were primarily controlled by three prevailing wind groups (winds from the northwest, north, and northeast), but showed complex changes between seasons and regions. The wind direction in the Taklimakan Desert is characterized by two characteristics of branch and steering, the branch line is swinging in the direction of the east and the west (81.5° E~84° E). The changes in wind speed were mainly caused by a decreased frequency of strong winds, precipitation, and urban development. However, the variation of wind speed had less impact on the desert environment than the variation of wind direction.

1 Introduction

The near-surface wind is a crucial component of atmospheric circulation, as it represents the interface between the atmosphere and Earth's surface. It is the main driving force that shapes the Earth's surface morphology. Variation in the wind regime has many consequences, such as changes in wind damage, vegetation propagation, dune fixation, the spread of desertification, and utilization of wind power (Azorin-Molina et al. 2016a; Zhao et al. 2015; Pryor et al. 2005; Paredes et al. 2017). Globally, near-terrestrial surface wind speeds have decreased significantly over the past few decades, and the rate of decrease has been faster for categories that include strong winds than for categories that include weak winds (Vautard et al. 2010), with confirmation of these trends observed in Italy (Pirazzoli and Tomasin 2003), China (Xu et al. 2006; Guo et al. 2011), the USA (Klink 1999; Pryor et al. 2009), the Netherlands (Smits et al. 2005), the Czech Republic (Brazdil et al. 2009), and Australia (McVicar et al. 2008). In contrast, winds above the world's oceans (Gulev and Grigorieva 2004) and at high latitudes (Aristidi et al. 2005; Lynch et al. 2004) have shown a greater increase for the category that includes the strongest winds. Guo et al. (2011) revealed that the weakened dust storms that have been described since the beginning of the twenty-first century in northern China have resulted from the decreased wind speed. In addition, the accumulation of haze in east-central China is also a direct result of reduced surface wind speeds, since weaker winds take longer to disperse the haze. Therefore, the study of wind regimes and their evolution represents an essential part of research on the Earth's surface system, particularly since climate change and variability influence key aspects of the surface environment.

Desert regions account for a third of the world's land area, and desert landscapes are the direct product of atmospheric circulation patterns. These phenomena have been studied in depth for northern China's deserts. In the middle reaches of

✉ Zhengyao Liu
liuzhengyaolzy@163.com

✉ Zhibao Dong
zbdong@snnu.edu.cn

[1] School of Geography and Tourism, Shaanxi Normal University, Xi'an 710119, China

[2] Key Laboratory of Desert and Desertification, Northwest Institute of Eco-Environment and Resources, Chinese Academy of Sciences, Lanzhou 730000, China

the Heihe Basin, the wind energy environment differs among regions (Zhang et al. 2010), and in the Kumtagh Desert, the resultant drift direction (RDD) differs between the northern and southern parts of the desert (Zhang and Dong 2014). The Badain Jaran Desert shows obvious local circulation patterns in the pattern of its megadunes and lakes (Zhang et al. 2013). The Taklimakan Desert is China's largest desert, and the second-largest desert in the world (Zhang 1984). Thus, changes in the environment of this region have serious impacts on local human survival and economic development. This desert has been well studied. For instance, Wu (1981) analyzed the desertification processes in this desert. Li et al. (1990, 1995) described the eolian landforms throughout the desert. Chen et al. (1995) studied the distribution of winds strong enough to transport sand. Zu et al. (2008) analyzed the characteristics of the near-surface wind regime before 2005. Rittner et al. (2016) explored the sources of the desert's sand and Huo et al. (2017) observed the particle sizes and fluxes of eolian sediment in the near-surface layer during sand and dust storms.

However, there have been few long-term studies of how the desert's wind regime has evolved (Cui et al. 2017). This makes eolian landform research difficult. To provide some of the missing data, we designed a study to quantify the changes in wind speed and drift potential (DP) in the Taklimakan Desert since 1965 (the date of the earliest widespread and reliable data). Our analysis examined the annual, seasonal, monthly, and regional changes in wind speed and DP. Based on our analysis, we mapped sand transport directions throughout the desert and their spatial and temporal variation. Based on these results, we discuss the factors that have influenced the changes. The results will support future studies of eolian geomorphology and will enrich our understanding of the wind environment of mid-latitude inland deserts.

2 Physiographic setting

The Taklimakan Desert (Fig. 1) is the world's largest mid-latitude desert, covering an area of 337,600 km^2 (Zhu et al. 1981). Wind and fluvial hydrology control the desert's current landscape. Geological evidence suggests that this desert evolved about 7 Ma ago in the center of the Tarim Basin, which is the largest inland basin in China and lies in the rain shadow of the Tibetan Plateau (Besler 1995). The desert then gradually expanded outward from the center.

It has plenty of sand sources and wind affect; three types of sand dunes exist, namely compound/complex crescent dunes and crescent chains, compound dome dunes, and compound/complex linear dunes; besides these three compound/complex types, single simple dunes are also distributed throughout the desert (Wang 2001). It also has a road of 519 km across the north and south. Climatically, the desert has a typical temperate continental climate, but because it lies in the rain shadow of the Tibetan Plateau, it is extremely arid; the average annual precipitation ranges from 100 mm in the east to less than 50 mm in the central desert (Yang 1992). The desert is surrounded by the Kunlun Mountains in the south and the Tianshan Mountains in the north. Under the impact of this physical setting, wind regimes become complicated. Despite the prevailing mid-latitude westerly atmospheric circulation pattern, the underlying topography and other wind systems, such as the winds produced by the Siberian high-pressure system, divert the wind flow locally.

3 Data and methods

To begin our research on the region's wind regime, we first selected appropriate wind data from weather stations distributed around the desert (Fig. 1). We chose these data sources to cover as much of the desert as possible, while providing continuous and high-quality data for as long a period as possible. Wind data, daily average air precipitation, daily average temperature, daily average sunshine time, and daily average sunshine percentage were obtained from the China Meteorological Data Service Center (http://data.cma.cn). In total, we identified 14 meteorological stations in or around the Taklimakan Desert that followed national standards for data collection and that could provide at least 50 years of data. The topography around each station is flat and open. The desert's remoteness and harsh environment have prevented researchers from maintaining stations inside the desert; so, coverage within the desert is limited and it was necessary to exclude some sites with missing data.

China's national standards prescribe wind data collection at a height of 10 m above the surface. This data included the daily average wind speed and the daily maximum wind speed, as well as wind directions. The standards define the daily average wind speed as the average of the values measured at 02:00, 08:00, 14:00, and 20:00 local time (which is equivalent to + 08:00 GMT). The data available at all 14 stations was collected between 1 March 1965 and 29 February 2016. We divided each year's seasons into spring, from March to May; summer, from June to August; autumn, from September to November; and winter, from December to February of the following year. The 14 stations were Tieganlike and Ruoqiang in the east; Yütian, Minfeng, and Qiemo in the south; Kashi, Shache, Pishan, and Bachu in the west; and Alaer, Akesu, Kuche, and Luntai in the north. Only one station (Tazhong) was available near the center of the desert.

Because some winds are not strong enough to entrain and transport sand, it was necessary to find a way to identify sand-moving winds capable of creating dune landforms (Xiao et al. 2018). Short-term intense winds are the main force that shapes eolian landforms

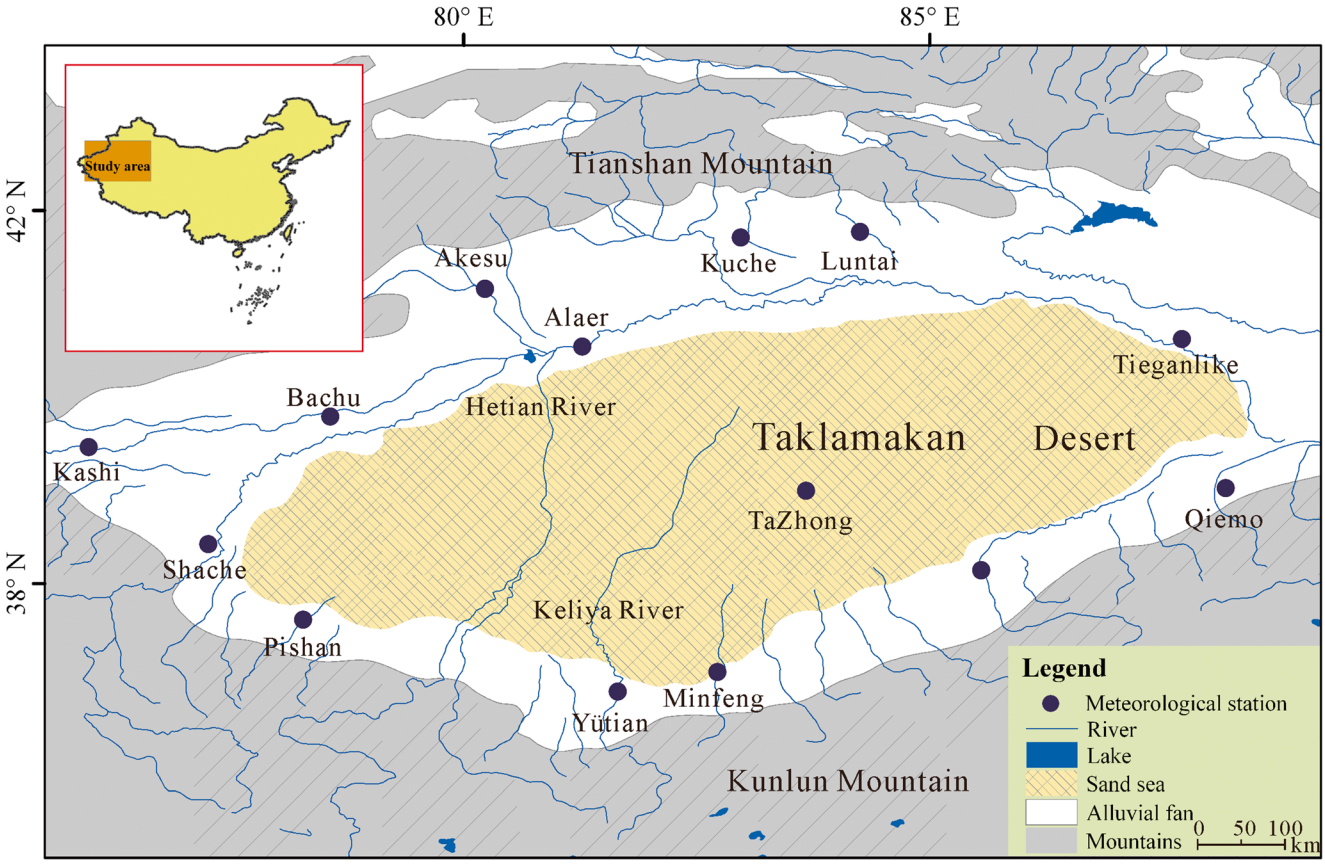

Fig. 1 Location of the study area and distribution of the meteorological stations in the Taklimakan Desert

(Bagnold 1941). In the present analysis, we used the maximum wind speed and wind direction to determine the frequency of intense winds (Cui et al. 2017).

From the original data, we selected the 95% percentile to remove extremes (Young et al. 2011) and improve homogeneity (Jiang et al. 2010). Using the remaining data, we performed regression analysis, spatial analysis with version 10.2 of the ArcGIS software (www.esri.com), wavelet analysis, and the Mann-Kendall mutation test in Matlab (https://www.mathworks.com) to analyze the temporal and spatial variation in the wind regime. Furthermore, we analyzed the variation in the drift potential (DP) proposed by Fryberger and Dean (1979):

$$\mathrm{DP} = U^2(U - U_t)\,t \tag{1}$$

where DP is the sediment's drift potential, which represents the relative rate of drift, and is calculated in vector units (VU); U is the measured 10-min mean wind speed at a height of 10 m above the surface, in knots; U_t is the threshold wind velocity (in knots) at which sand transport begins, which was 6 m s^{-1} in this paper (Geng 1985; Wang et al. 2002); and t is the proportion of the recorded time during which the wind speed exceeded the threshold velocity (Fryberger and Dean 1979).

DP quantifies the long-term wind and sand activity and is the most widely used index for this purpose. In addition to wind speed, the wind direction is important because it determines sand sources and migration directions (Zhu et al. 1981). DP can be used to reflect the magnitude of the sand transport capacity in each wind direction and to identify the prevailing sand transport directions, and RDD represents the resultant direction of the sand transport. Both parameters are usually presented in a wind-rose diagram that summarizes the distribution of sand transport and its direction. The length of each arrow in the wind-rose diagram represents the relative magnitude of sand transport in that direction.

Using vector mathematics, we also calculated the resultant drift potential (RDP), the directional variability (RDP/DP), and RDD. Fryberger and Dean (1979) also proposed a classification for the wind energy environment based on the calculated DP: low energy (DP < 200), intermediate energy (200 < DP < 400), and high energy (DP > 400). We divided the observed wind regimes into five types according to the characteristics of the wind-rose diagram and three types based on the value of RDP/DP.

To discuss the impact of wind energy changes on the desert environment, we quantified the vegetation change using the normalized-difference vegetation index (NDVI), a widely used index of surface greenness that is derived from

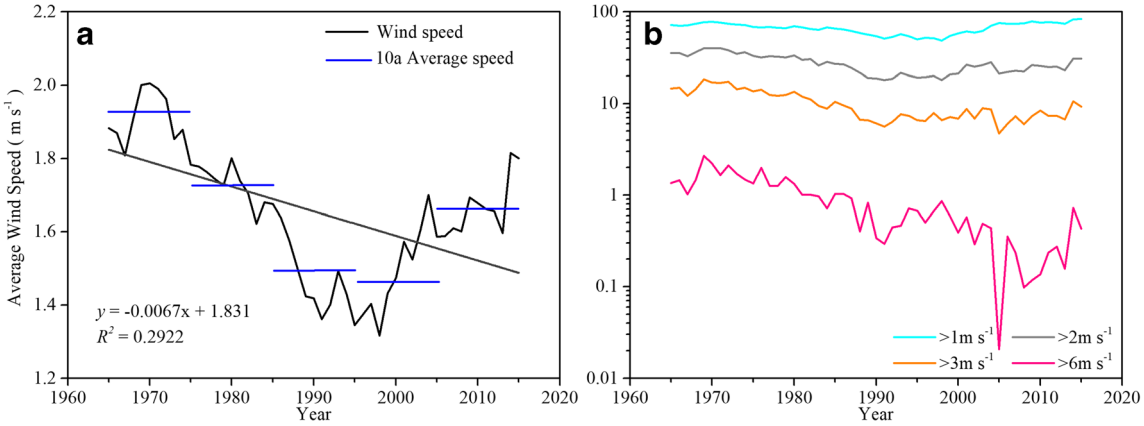

Fig. 2 **a** Variations at annual and decadal time scales of wind speed in the Taklimakan Desert during 1965–2015. **b** Wind speed distribution evolution: respectively for the frequency (in % per year) of winds stronger than 1, 2, 3, and 6 m s^{-1}. The numbers represent all stations in the domains taken together as well as all days and seasons

multispectral remotely sensed images (Mason et al. 2008; Xu et al. 2016). We obtained MODIS NDVI data from 2000 to 2015 from Land Processes Distributed Active Archive Center (https://lpdaac.usgs.gov/), at a resolution of 500 m and a temporal resolution of 16 days. We synthesized the 16 years of data by season and calculated the annual value as the average NDVI value for the 16-year period. We then mapped the spatial distribution across each part of the study area.

4 Results and analysis

4.1 Temporary variation of wind speed

The average annual wind speed in the Taklimakan Desert since 1965 was 1.7 m s^{-1}.

Figure 2a shows the overall trend, which can be divided into two sections. Wind speeds decreased from 1965 to 2000, then increased until the end of the study period. The averaged decade wind speeds have a similar trend as annual wind speed, which decreased from 1965 to 2004, and then increased: 1.9 m s^{-1} (1965–1974), 1.7 m s^{-1} (1975–1984), 1.5 m s^{-1} (1985–1994), 1.5 m s^{-1} (1995–2004), and 1.6 m s^{-1} (2005–2015). A slight increase occurred in the twenty-first century. From the evolution of wind velocity distribution (Vautard et al. 2010), we find that the frequency of wind speeds ≥ 1 m s^{-1} was the highest (66.7%) and there is no clear change in this speed Fig. 2b. Further accurate analysis, the frequencies of wind speeds > 2 m s^{-1} and > 3 m s^{-1} were 40.9% and 36.1%, respectively, representing a slight decrease. Although the frequency of wind speeds > 6 m s^{-1} was only 8.7%, the fluctuation was comparatively highest and consistent with the overall wind speed change; it was the main factor of the change in the overall average wind speed.

We also analyzed the data for each season (Fig. 3). The average wind speed was strongest in spring (2.1 m s^{-1}), followed by that in summer (1.9 m s^{-1}), autumn (1.4 m s^{-1}), and winter (1.2 m s^{-1}). From the monthly data at each meteorological station shown in Fig. 3b, the average wind speed was strongest in May (2.2 m s^{-1}) and weakest in November (1.1 m s^{-1}). With respect to wind speed change, the rate of decrease in spring (Fig. 4a) was the largest, followed by

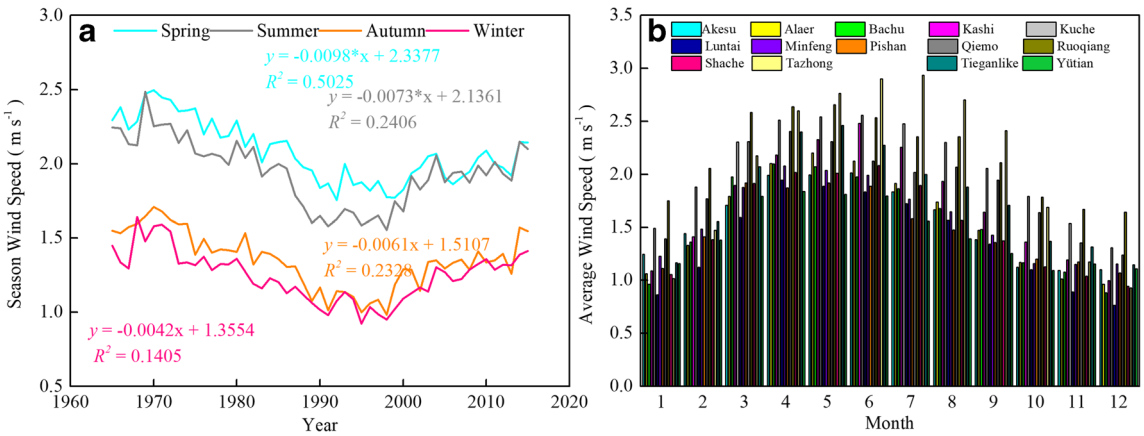

Fig. 3 **a** Seasonal variations of wind speed in the Taklimakan Desert from 1965 to 2015. **b** Monthly changes of wind speed at each meteorological station

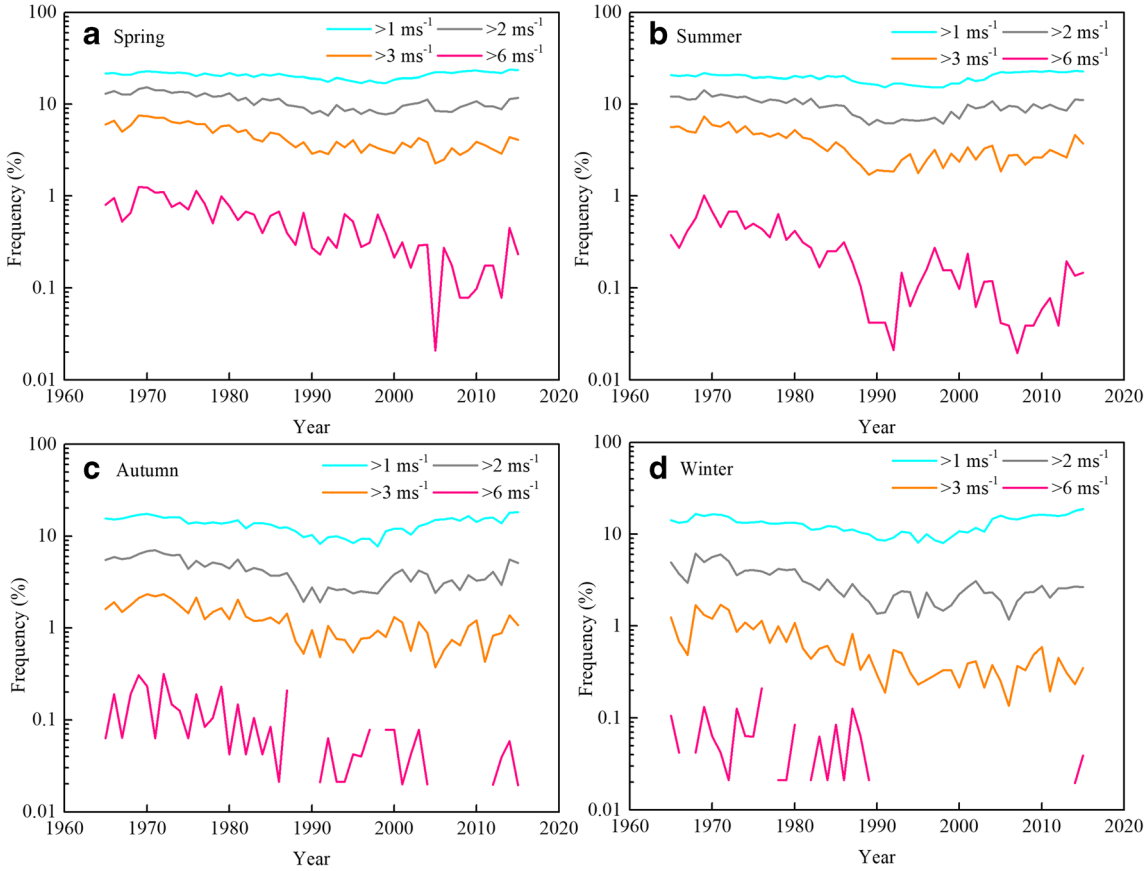

Fig. 4 Evolution of the wind speed distribution for the frequency of winds stronger than 1, 2, 3, and 6 m s^{-1} for **a** spring, **b** summer, **c** autumn, and **d** winter

summer (Fig. 4b), autumn (Fig. 4c), and winter (Fig. 4d). However, the recovery of wind speed in spring was not as strong as that in other seasons after the year 2000.

Figure 4 shows the frequency distributions of the wind speeds. As in the overall wind speed data in Fig. 2b, wind speeds > 1 m s^{-1} accounted for the largest proportion of the winds, and this proportion was relatively stable. The overall trend throughout the year showed that wind speed first decreased and then increased, with the greatest increase in winter. The frequency of wind speeds > 2 m s^{-1} and > 3 m s^{-1} in spring and summer first decreased and then increased; in autumn, they first decreased, and then increased with fluctuation, versus nearly continuous decreases in winter. The proportion of winds with a wind speed > 6 m s^{-1} in spring decreased before 1990, and then stabilized, with fluctuation. Summer showed a similar pattern, but with the steady decrease ending around 1990. Autumn showed a roughly continuous decrease, though with missing data, and winter showed no clear pattern due to high variation and missing data. The wind speed greatly increased in the twenty-first century, and the frequency even surpassed the maximum of the 1960s after 2005.

The average wind speed from 1965 to 2015 was highest (2.2 m s^{-1}) at the Ruoqiang station, followed by the Tazhong and Kuche stations, whose average wind speed was 2.1 m s^{-1}; the lowest average wind speed was 1.4 m s^{-1} at the Tailun site. When we grouped the stations by region and analyzed the data separately for each region, the average wind speed from 1965 to 2015 was highest in the eastern region, followed by the southern, northern, and western regions. Figure 5a shows that the wind speed decreased from 1965 to somewhere between 1990 and 1995 in all regions. However, the average wind speed increased in every region except the east after 1995. Figure 5b shows the wind speed frequency distribution in every region. There was no obvious difference in the trend over time for the four regions in the proportion of the winds with a wind speed > 1 m s^{-1}, but the actual proportions differed by a factor of nearly 2 times between regions. The difference between regions increased for higher wind speeds, especially for the winds with an average wind speed > 6 m s^{-1}. Although the frequency of winds with a wind speed > 6 m s^{-1} in the east increased slightly around 1995, it continued to decrease thereafter. In the other three regions, the frequency of winds with a wind speed > 6 m s^{-1} increased in the twenty-first century, although their proportions for this speed category remained less than that in the east. The average wind speeds in the eastern and southern regions of the

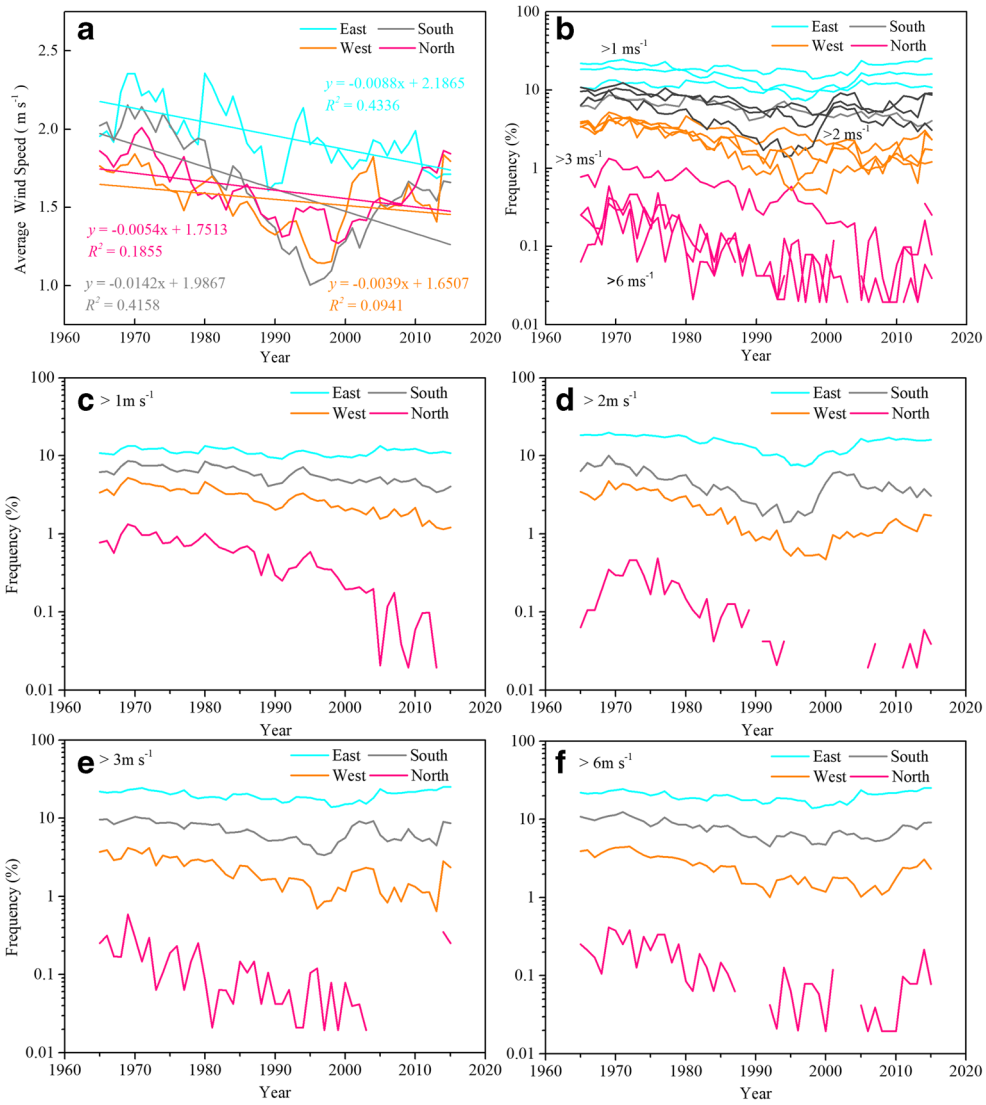

Fig. 5 Evolution of the average wind speed from 1965 to 2015 for the eastern, southern, western, and northern parts of the study area. **b** Frequency distributions for the frequency of winds stronger than 1, 2, 3, and 6 m s^{-1} in the four regions; the details are as follows, **c**, **d**, **e**, and **f**

Taklimakan Desert were greater than those in the western and northern regions, and this spatial difference was mainly determined by the proportion of the wind speeds > 6 m s^{-1}.

4.2 Spatial and temporal variation of drift potential

Figure 6 shows the spatial distribution of the wind speeds, based on kriging interpolation between the meteorological stations. Early researchers adopted 2-min and 10-min averages, 10-min maximums, and 1-h instantaneous maximum wind speeds to calculate DP. We chose the maximum 10-min wind speed per day because it is more accurate, and removed extreme values to improve homogeneity for the calculation of DP. Previous research suggested that the dominant RDD in the Taklimakan Desert was towards the SW, SSW, and E, under a low-energy wind environment with wide unimodal wind regimes (Zhu et al. 1981; Zu et al. 2005).

4.2.1 Temporal variation of drift potential

DP for the Taklimakan Desert for the year as a whole averaged 189 VU from 1981 to 2015 (Fig. 7). The annual RDP averaged 68 VU, and RDP/DP averaged 0.36, indicating an intermediate ratio that reflects a strongly bimodal wind regime. NW and NE were the main wind directions. The average annual RDD was 335°, which indicates that the main wind direction in the region was from the NW.

Based on the availability of data, we divided the study period into three 10-year periods (1981 to 1990, 1991 to 2000, 2001 to 2010) and one 5-year period (2011 to 2015). DP and RDP decreased from 1981 to 2010, then increased from 2011 to 2015. RDP/DP ranged from 0.27 to 0.64 and showed no clear trend. The main directions of sand transport were SW, SSW, and E. DP in the SSW direction gradually decreased, whereas in the SE

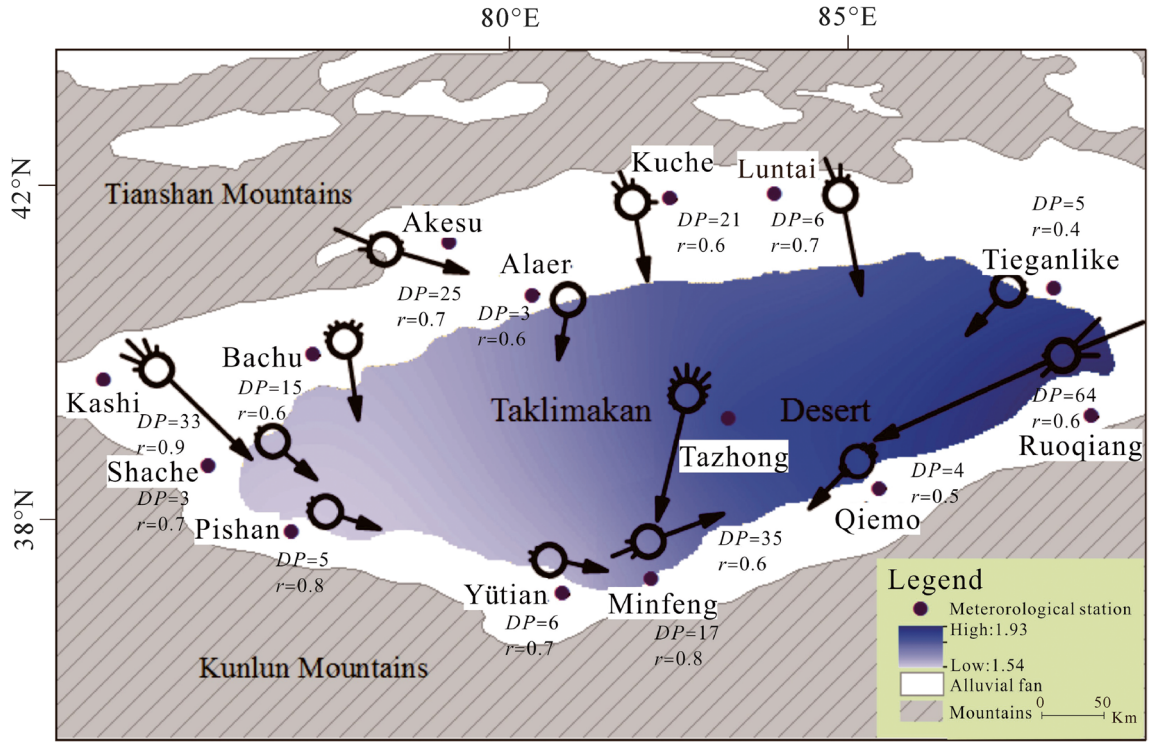

Fig. 6 Spatial distribution of the average wind speed from 1965 to 2015 based on kriging interpolation between meteorological stations in the Taklimakan Desert. Circles and arrows show the wind-rose diagram for each station. DP, drift potential; *r*, the directional variability

direction, it first decreased and then increased. RDD was mostly between 138° and 182°.

The maximum *DP* occurred in the spring, followed by summer, autumn, and winter. RDP was highest in spring, followed by summer, autumn, and winter. RDP/DP ranged from 0.33 to 0.43. In spring, autumn, and winter, SE and SW were the most prominent sand transport directions, with strongly bimodal wind regimes, and RDD was SSE. Although the summer wind regimes were complex, there were winds from the NW, W, SW, and NE, and RDD was SSE. For the spring, DP for winds from the NW first decreased and then increased, whereas DP for winds from the NE gradually decreased, and RDD moved from SSE to SSW and then back to SSE. In the summer, DP for winds from the SW, W, and NE decreased greatly, whereas DP for winds from the NW and N increased during the twenty-first century. In the autumn, DP was smaller than that in the spring and summer. From 1981 to 2000, DP for winds from the NW, WNW, and NE decreased, and RDD changed from S to SSE. Since 2000, the transport potential for winds from the NW decreased, and RDD returned to SSE. RDP was lowest in winter, and DP increased and then decreased, with RDD fluctuating between east and west. DP showed complicated patterns in both direction and size. Before the 2010s, the wind in the direction of sediment transport decreased greatly in strength, but increased somewhat thereafter.

4.2.2 Spatial variation of drift potential

Figure 8 shows the spatial distribution of the DP, RDP, RDD, and RDP/DP values throughout the study period. DP was largest in the east in all periods except 2011 to 2015, generally followed by the north, south, and west, but all four regions had a low-wind-energy environment (< 200 VU). For the eastern region, DP was mainly for winds from the NE and exhibited a wide unimodal wind regime. For the northern region, DP was mainly for winds from the NNW and WNW and showed an acute bimodal wind regime. For the western region, DP was focused on winds from the NW and was a narrow unimodal wind regime. For the southern region, DP was mainly for winds from the NNW, and it exhibited a wide unimodal wind regime. The RDP/DP values of the four regions ranged between 0.36 and 0.80, which represent intermediate values. Over time, the direction of sediment transport generally showed relatively little variation, but with a large clockwise shift in the western and northern regions after 2010, and the magnitude of DP generally decreased continuously, except for increases for the western and northern regions after 2010.

Figure 9 illustrates the spatial variation in wind directions based on averages from 1971 to 2015. RDD reflects the net flow direction created by the effective sand-moving wind, and the size of the arrow indicates the size of the DP. The airflow appears to form two distinct regions on either side of 83.5° E: the western region was more complex, but winds originated

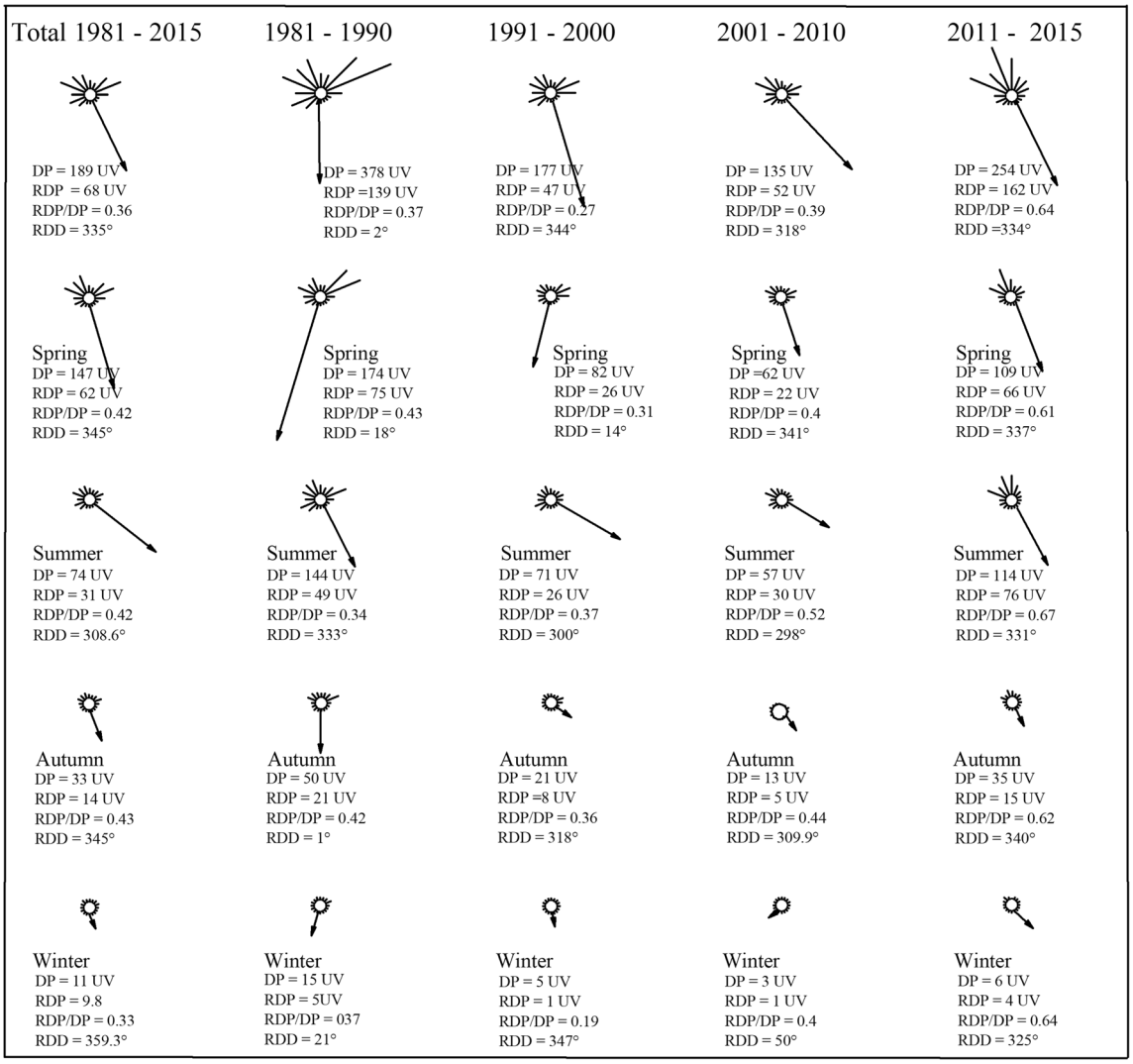

Fig. 7 Temporal variation of the wind regime (DP, drift potential; RDP, resultant drift potential; RDP/DP, directional variability; RDD, resultant drift direction) in the Taklimakan Desert from 1981 to 2015

mainly from the NW to N, whereas the eastern region was simpler, and the winds originated mainly from the N to NE.

Figure 10 shows the spatial distribution of RDD during each season. Although the overall pattern is similar to that in Fig. 9, with a division of the airflow into distinct regions, the position of the division changes between seasons. It moves westward early in the year, then moves eastward later in the year. The division for the spring flow field was near 81.5° E, with airflow west of this line primarily originating from the NW and east of this line mainly from the NE. The flow field in summer is more complex, with division into three regions divided at roughly 81.5° E and 84.0° E. West of 81.5° E, winds originated mainly from the NNW, whereas east of 84° E, winds originated mainly from the NE; between these two regions, winds originated primarily from the N. The autumn air flow in the desert returns to two distinct regions, with the division near 81° E. West of this line, the flow is predominantly from the NW, and east of the line, it is primarily from between E and NE. In winter, the airflow returns to a pattern similar to the spring pattern, with two distinct regions.

4.3 The impact of wind variation on the environment

Plant productivity in desert areas is more sensitive to the environment than it would be in wetter areas. The desert areas in our study area have low vegetation cover and are dominated by partially to fully active dunes. The wind regime is the main driving force for the formation and evolution of these eolian sandy landforms, and vegetation growth and cover respond to these changing landforms. Our analysis of remote sensing images let us monitor changes in vegetation cover during the study period, and compare this with the temporal and spatial variation of the wind energy environment in the Taklimakan Desert (Fig. 11). Figures 5 and 7 suggest that the wind speed

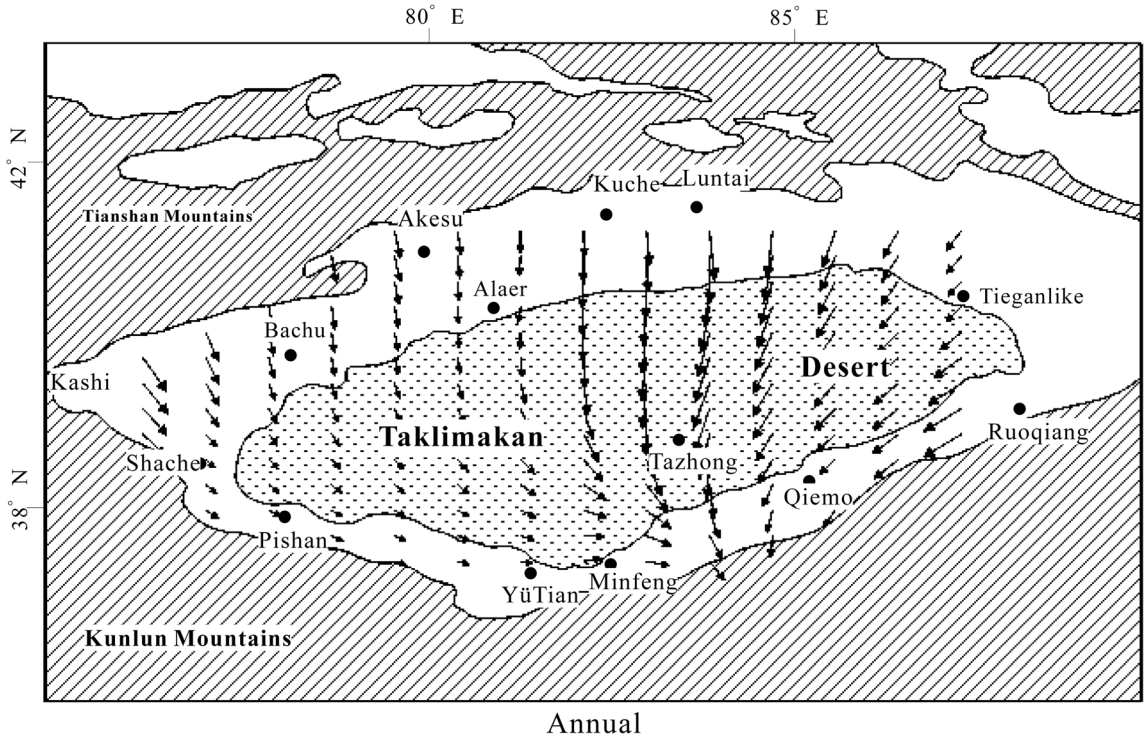

Fig. 8 Spatial variation of the wind regime in the Taklimakan Desert from 1981 to 2015. DP, drift potential; RDP, resultant drift potential; RDD, resultant drift direction; RDD/DP, directional variability

has increased significantly in much of the study area since 2010, with DP increasing by an average of 88.1% throughout the study region. In the northern part of the study area, *DP* increased to nearly two times the 2010 level, and vegetation cover decreased. In the southern part, both DP and vegetation cover increased. DP did not increase significantly in the west, but the wind direction changed greatly. Vegetation cover increased in much of the southwestern part, with a significantly increasing trend near the relatively wet areas around the Hetian River and the Keliya River. However, as the wind speed is much higher in spring and summer than in autumn and winter, the vegetation growth rate is slightly lower than that in autumn and winter. DP increased least in the spring, and the vegetation cover slightly increased in the northeastern and southwestern parts of the desert, but significantly decreased in the center of the desert. In autumn, the differentiation was greater, with the NW wind's DP increasing to nearly three times the summer level, but the vegetation cover in the west increased, although 20.7% of the area showed significantly decreased vegetation cover. In winter, RDD changed greatly, with the NE wind weakening and NW wind strengthening. The vegetation cover in the west increased significantly, but for the study area as a whole, it decreased, despite the slight increase in the west. In general, the increased wind energy had little obvious impact on vegetation cover, which agrees with previous research results in semi-arid northern China (Mason et al. 2008). However, the change of wind direction had a greater impact on the increase of vegetation coverage and the landform of desert surface.

4.4 Wavelet analysis and Mann-Kendall mutation test

We performed wavelet analysis for the wind speeds in the Taklimakan Desert from 1965 to 2015 (Fig. 12a), and found alternation between positive phases (solid lines) and negative phases (dashed lines). This represents alternation between periods with a high average wind speed and periods with a low average wind speed. The region's average wind speed had two peaks that corresponded to time scales of 8 and 27 years. However, because of the short period covered by our study, it will be necessary to confirm the existence of the 27-year cycle over a longer monitoring period.

Figure 12b shows the results of the Mann-Kendall mutation test (Mann 1945; Kendall 1975). The UF curve for the Taklimakan Desert from 1965 to 2012 showed that the average annual wind speed in the Taklimakan Desert has decreased significantly since the 1960s; the M-K statistic exceeded the line that represents significance at $p < 0.05$ in 1981 and exceeded the $p < 0.001$ significance level in 1986. According to the location of the intersection of the UF and UB curves, the annual mean wind speed in the Taklimakan Desert decreased significantly starting in 1976.

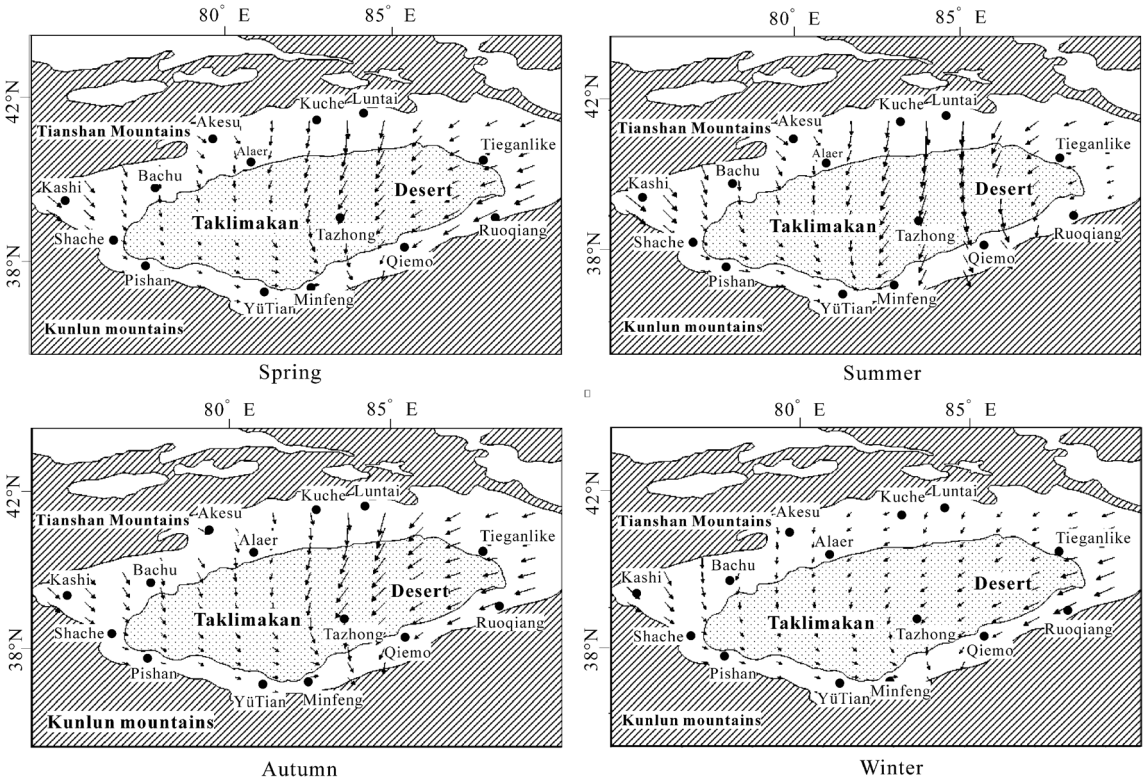

Fig. 9 Mean sand drift direction in the Taklimakan Desert from 1971 to 2015. Longer arrows represent stronger drift

5 Discussion

Wind energy is of concern in the context of global warming both because it is a new energy source that can reduce fossil fuel use and because it is an important driving force in environmental change. In a complex environment, changes of wind direction and speed are complex and variable. The inland desert area of northwestern China is strongly affected by its wind energy regime, which has shaped its eolian landscape and its vegetation. In the present study, we provided more information about the region's wind regime and its temporal and spatial variation.

5.1 Wind speed change

Von-Axe (1975) estimated that the wind energy available on Earth is around 106 MW, and that wind energy resources in arid regions are the dominant ones. However, numerous studies have shown that wind speeds have decreased since the start of the twenty-first century (Klink 1999; Pryor et al. 2009; McVicar et al. 2008; Aristidi et al. 2005). According to our analysis of 50 years of wind regime data, the average wind speed in the Taklimakan Desert was 1.7 m s^{-1}, and gradually decreased during the first 10 years of the study period, abruptly decreased in 1976, and then increased during the twenty-first century. This finding is similar to the results of Fu et al. (2011) and Guo et al. (2011), who detected similar oscillation periods to those in Fig. 12. The maximum average wind speed appeared in the spring and May, with the weakest winds in the winter and December. The largest decrease in the mean wind speed appeared in the spring, particularly for winds with a speed > 6 m s^{-1}.

5.2 Variation in DP and RDD

Previous research suggests that the Taklimakan Desert was an environment with high wind energy in the 1960s and 1970s, but changed to an environment with low wind energy in the 1990s (Zu et al. 2005; Wang et al. 2007). This agrees with the present results, which show a gradual decrease in the mean wind energy to produce an environment with a low wind energy between 1981 and 2010. The DP in the study area first decreased and then increased, and the wind directions were mainly from the NW, NE, and N. The DP for winds from the NE gradually decreased, whereas DP for the winds from the NW and N first decreased and then increased. DP was strongest in the spring, followed by summer, autumn, and winter. The largest DP values appeared in the eastern region, followed by the northern, western, and southern regions. Winter and spring winds are mainly influenced by the anti-cyclones of Mongolia–Siberia, which create a strong NE wind, whereas summer and autumn winds in the western region of the desert

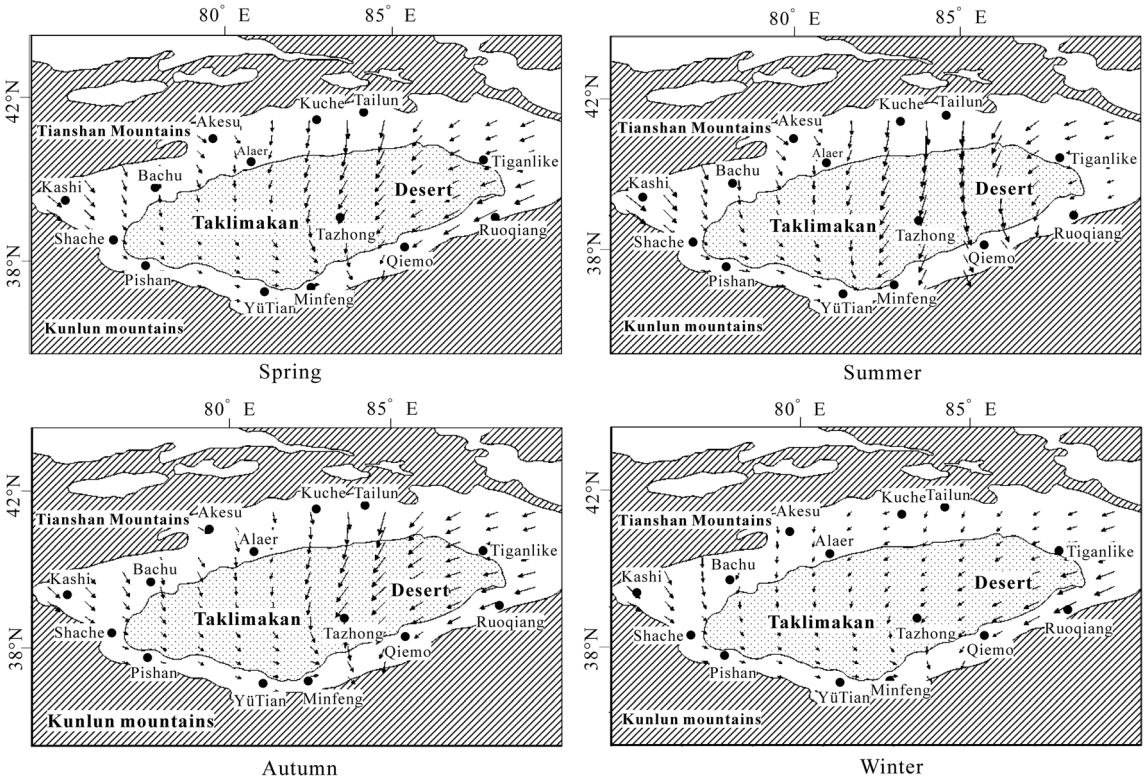

Fig. 10 Season sand drift direction in the Taklimakan Desert from 1971 to 2015. Longer arrows represent stronger drift

are dominated by the prevailing westerlies and by NW and N winds from the Tianshan Mountains. RDP was mainly affected by the decrease in the number of events with high wind speed from the NW and NE, although the increase in RDP in 2000 mainly resulted from increased wind strength from the NW. A previous study showed that the direction of the dunes (the dune ridge lines) in the Tengger Desert, near our study area, was strongly related to the wind speed and direction (Lü et al. 2013). The change of DP since 1965 is therefore likely to have strongly influenced the Taklimakan Desert landscape. Wang (2001) showed that the strength of the East Asian monsoon circulation has been decreasing since the 1970s. However, the increasing wind speed we observed since 2000 may indicate that the strength of the atmospheric circulation is beginning to increase again.

5.3 Possible causes of observed wind speed trends

The reasons for the change of terrestrial surface winds include precipitation, temperature, and other factors (Zhang et al. 2007; Yang et al. 2009; Vautard et al. 2010; Azorin-Molina et al. 2016b; Zheng et al. 2017). This paper used SPSS20.0 software for the wind speed and air precipitation, temperature, sunshine time, sunshine percentage, and other factors influencing the correlation analysis.

5.3.1 Precipitation

Wind speed and precipitation exhibited a strong and significant correlation. When we performed Mann-Kendall trend analysis, the precipitation z value was 1.776, versus −4.482 for wind speed, indicating that precipitation increased and wind speed decreased, which is consistent with the negative correlation between these variables. It is possible to explain this relationship based on energy balance and vegetation factors. Precipitation increases soil moisture, which leads to both greater absorption of solar energy by the wet soil, which reduces the energy reflected by the surface to drive the wind; it also increases plant growth, creating a rough boundary layer that slows the wind. This phenomenon would be supported by changes in evapotranspiration in the Taklimakan Desert, which decreased during most of the period since 1965, before increasing again after 1996, which agrees with the trend for wind speed. However, the restoration of vegetation cover in the Taklimakan Desert has been slow (Li 2013), which may be why the wind speed has not continued to decline.

5.3.2 Temperature

Since the 1960s, a warming climate has been observed both globally (at 0.13 °C per decade) and in China (0.23 °C per decade), but has occurred even faster in the Taklimakan Desert temperature (0.26 °C per decade). From 1965 to the 1990s, the

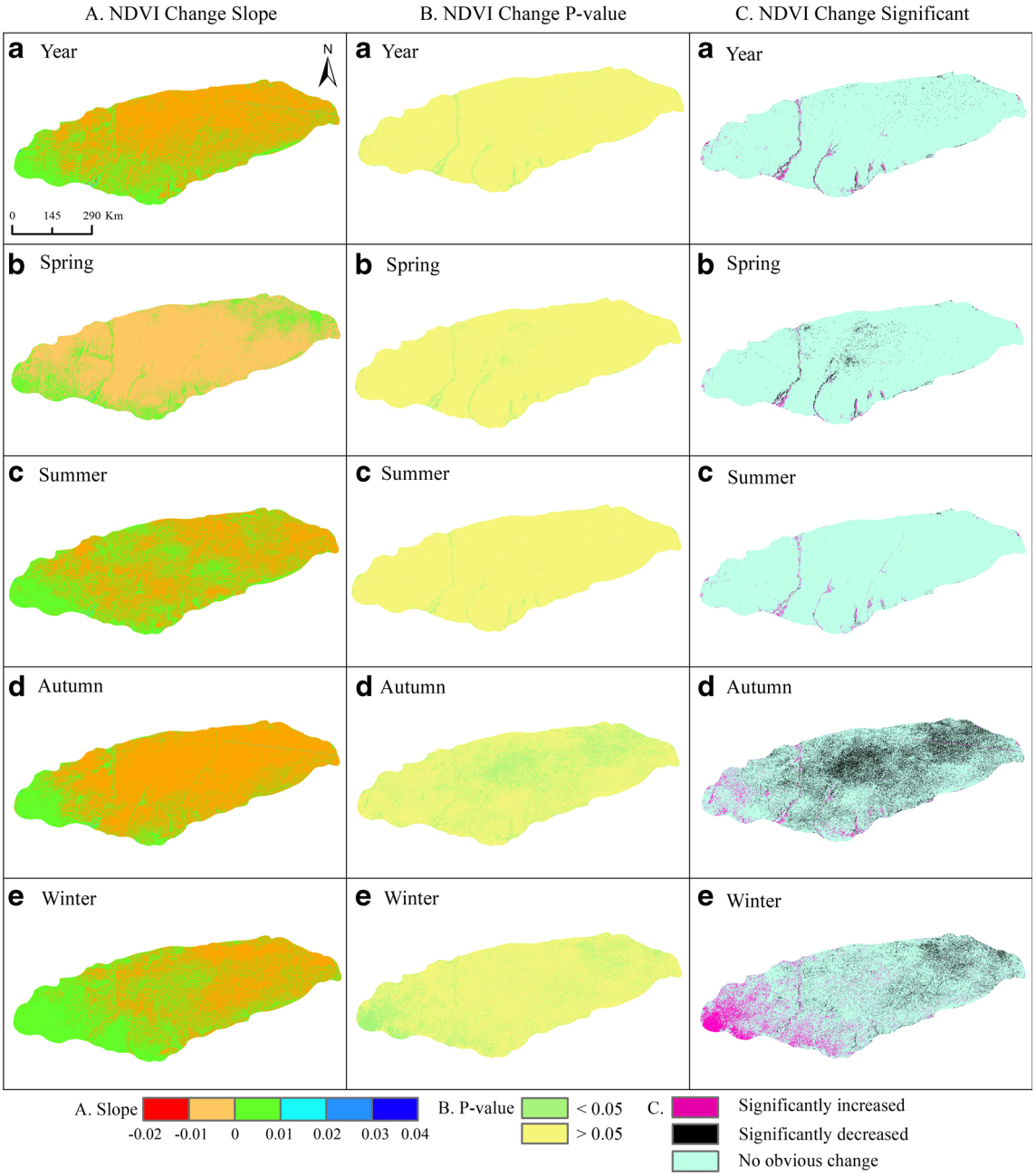

Fig. 11 The spatial and temporal variations of the normalized-difference vegetation index (NDVI) in the Taklimakan Desert from 2000 to 2015 based on MODIS NDVI images with 500-m resolution. (A) Rates of change of NDVI. (B) Significance levels for the changes in (A). (C) Significant increases and decreases. All data are averages for the study period

temperature has been slowly increasing (Pu et al. 2010), while the wind speed has decreased by an overall average of 0.19 m s^{-1} per decade, which is at the high end of the range reported for northern China, from 0.15 to 0.19 m s^{-1} per decade (Tian 2012). Yang et al. (2012) found that the sea-level pressure and the near-surface temperature difference between continental Asia and the Pacific Ocean have decreased significantly, while the East Asian pressure trough has shifted eastward and northward while simultaneously weakening. The strengths of the East Asian winter and summer monsoons have also been decreasing (Jiang and Wang 2005). The combination of these factors has resulted in decreasing mean wind speed in China. However, the temperature increase has accelerated since the late 1990s, simultaneously with an increase of the mean wind speed by 0.14 m s^{-1} per decade. This appears to be because the sudden warming that began in the 1990s led to an increase in the pressure differences that drive the wind, thereby increasing the wind speed, although the wind speed

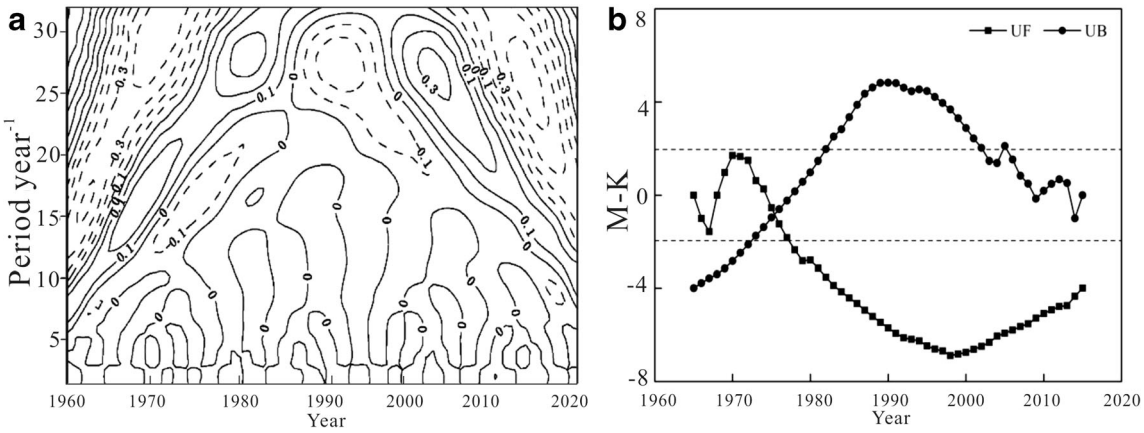

Fig. 12 Changes of wind speed characteristics in the Taklimakan Desert over the past 50 years. **a** Matlab wavelet transforms. Positive phases are denoted by solid lines and negative phases are denoted by dashed lines. **b** Results of the Mann-Kendall mutation test. M-K, the Mann-Kendall statistic; UF, plus sequence statistics; UB, contrary sequence statistics. The dashed horizontal lines represent significance at $p < 0.05$

has not yet recovered to its peak at the start of our study period. He et al. (2011) found that wind speed change in the Taklimakan Desert has strongly influenced wind erosion of soils and the surface roughness.

5.3.3 Other factors

Zhao et al. (2015) noted that the construction of urban land can decrease wind speeds because the tall buildings create strong obstacles to the wind. Dai (2012) studied the changes in urban land around the Taklimakan Desert and found that changes from agricultural land and ecological land to urban land increased the topographic roughness, thereby slowing the wind. However, paved urban areas tend to be smoother than the surrounding landscape, reducing the friction and increasing wind speeds compared with natural terrain.

6 Conclusion

The main findings in our long-term (1965 to 2015) study of wind regimes in the Taklimakan Desert are as follows:

1. The wind speed in the Taklimakan Desert during this 50-year period averaged 1.7 m s^{-1}; the average wind speed decreased from 1965 to 2000 and then increased thereafter, but has not yet recovered to the 1965 level.
2. The average wind speed was highest in the spring. The increased wind speed from 2000 to 2015 was mainly caused by increased wind speeds for the autumn winds. Changes in the proportion of winds with a wind speed > 6 m s^{-1} were the main factor that changed the average wind speed. The eastern region had the highest wind speeds, followed by the southern, northern, and western regions. These changes were mainly determined by changes in the frequency of winds with a speed >6 m s^{-1}.
3. The Taklimakan Desert has both unimodal and bimodal wind regimes, and the wind field for the whole region tended to be divided into two sub-regions. RDP decreased during the first part of the study period and then increased, with the main winds coming from the N, NW, and NE. RDD mainly ranged from 138° to 182°, and DP was largest in the spring. DP was largest in the eastern region, followed by the northern, western, and southern regions. The variation of wind speed may have had less impact on the desert environment than changes in the wind direction.
4. The average wind speed decreased gradually until 1976, when it suddenly decreased. There appear to be cycles of 8 years during which wind speed increases and then decreases.

Acknowledgements We gratefully acknowledge the China Meteorological Data Service Center for the supply of meteorological data and Land Processes Distributed Active Archive Center for the supply of the NDVI data.

Funding This work was supported by the Fundamental Research Funds for the Central Universities of China (GK201704012 and GK201903073) and National Natural Science Foundation of China (41571008 and 41871011).

References

Aristidi E, Agabi K, Azouit M, Fossat E, Vernin J, Travouillon T, Lawrence JS, Meyer C, Storey JWV, Halter B, Roth WL, Walden V (2005) An analysis of temperatures and wind speeds above dome

c, Antarctica. Astron Astrophys 415(2):739–746. https://doi.org/10.1051/0004-6361:20041876

Azorin-Molina C, Guijarro JA, McVicar TR, Vicente-Serrano SM, Chen DL, Jerez S, Espirito-Santo F (2016a) Trends of daily peak wind gusts in Spain and Portugal, 1961-2014. J Geophys Res Atmos 121(3):1059–1078. https://doi.org/10.1002/2015JD024485

Azorin-Molina C, Vicente-Serrano SM, McVicar TR, Revuelto J, Jerez S, Lopez-Moreno J (2016b) Assessing the impact of measurement time interval when calculating wind speed means and trends under the stilling phenomenon. Int J Climatol 37(1):480–492. https://doi.org/10.1002/joc.4720

Bagnold RA (1941) The physics of blown sand and desert dunes. William Morrow & Company, New York, pp 167–187. https://doi.org/10.1007/978-94-009-5682-7

Besler H (1995) The keriya dunes in the taklimakan sand sea: sediment logical evidence for a polygenetic evolution, Die Erde 126:205–222

Brazdil R, Chromá K, Dobrovolný P, Tolasz R (2009) Climate fluctuations in the Czech Republic during the period 1961-2005. Int J Climatol 29:223–242. https://doi.org/10.1002/joc.1718

Chen WN, Dong ZB, Yang ZT, Han ZW, Zhang JK, Zhang ML (1995) The threshold wind velocity in the Taklimakan Desert. Acta Geograph Sin 4(7):361–367. https://doi.org/10.11821/xb199504008

Cui X, Dong Z, Sun H, Li C, Xiao FJ, Liu ZY, Song SP, Li XL, Xiao N, Xiao WQ (2017) Spatial and temporal variation of the near-surface wind environment in the dune fields of northern China. Int J Climatol 38(5):2333–2351. https://doi.org/10.1002/joc.5338

Dai R (2012) Anwaer Maimaitiming. Analysis of spatial structure change of urban land for construction in Southern City of Xinjiang. J Yili Normal Univ (Nat Sci Ed) 3(1):42–47

Fryberger SG, Dean G (1979) Dune forms and wind regime. In: McKee ED (ed) A study of global sand seas. Professional Paper No, vol 1052. U.S. Geological Survey, Washington, pp 137–169

Fu G, Yu J, Zhang Y, Hu S, Ouyang R, Liu W (2011) Temporal variation of wind speed in China for 1961-2007. Theor Appl Climatol 104(3–4):313–324. https://doi.org/10.1007/s00704-010-0348-x

Geng KH (1985) Climatic study on sand-blowing wind in desert regions in China. J Desert Res 5(1):16–26

Gulev SK, Grigorieva V (2004) Last century changes in ocean wind wave height from global visual wave data. Geophys Res Lett 31(24):357–370. https://doi.org/10.1029/2004gl021040

Guo H, Xu M, Hu Q (2011) Changes in near-surface wind speed in China: 1969–2005. Int J Climatol 31(3):349–358. https://doi.org/10.1002/joc.2091

He Q, Yang XH, Mamtimin A, Tang SH (2011) Impact factors of soil wind erosion in the center of Taklimakan Desert. J. Arid. Land, 3(1):9–14. https://doi.org/10.3724/SP.J.1227.2011.00009

Huo W, He Q, Yang F, Yang X, Yang Q, Zhang F, Mamtimin A, Liu XC, Wang MZ, Zhao Y, Zhi XF (2017) Observed particle sizes and fluxes of aeolian sediment in the near surface layer during sand-dust storms in the Taklamakan desert. Theor Appl Climatol 130(3–4):735–746. https://doi.org/10.1007/s00704-016-1917-4

Jiang DP, Wang HJ (2005) The natural property of decadal weakening of east Asian summer monsoon in the late 20th century. Chin Sci Bull 50(20):2256–2262. https://doi.org/10.1360/982005-36

Jiang Y, Luo Y, Zhao Z, Tao S (2010) Changes in wind speed over China during 1956–2004. Theor Appl Climatol 99(3–4):421–430. https://doi.org/10.1007/s00704-009-0152-7

Kendall MG (1975) Rank correlation methods. Charles Griffin, London

Klink K (1999) Trends in mean monthly maximum and minimum surface wind speeds in the coterminous United States, 1961 to 1990. Clim Res 13(3):193–205

Li XT (2013) Sparse vegetation coverage information extraction and analysis of temporal and spatial variation of arid desert in XINJIANG. North West Agriculture and Forestry University, Xi'an

Li BS, Dong GR, Ding TH, Jin C, Jin HL, Gao SY (1990) Several arguments for the aeolian geomorphology in the eastern Taklimakan Desert. Chin Sci Bull 35(23):1815–1818. https://doi.org/10.1007/BF02919267

Li BS, Dong GR, Zhang JK, Lin S, Jin HL, Chen HZ, Wen XL, Wang Y, Zhu YZ (1995) Division and recognition of the aeolian facies belts in the Taklimakan Desert and areas to its south. Acta Geol Sin 69(1):78–86

Lü P, Narteau C, Dong ZB, Zhang ZC, Pont SC (2013) Emergence of oblique dunes in a landscape-scale experiment. Nat Geosci 7:99–103. https://doi.org/10.1038/ngeo2047

Lynch AH, Curry JA, Brunner RD, Maslanik JA (2004) Toward an integrated assessment of the impacts of extreme wind events on barrow, Alaska. Bull Am Meteorol Soc 85(2):209–221. https://doi.org/10.1175/BAMS-85-2-209

Mann HB (1945) Nonparametric tests against trend. Econometrica 13(3):245–259. https://doi.org/10.2307/1907187

Mason JA, Swinehart JB, Lu H, Miao X, Cha P, Zhou Y (2008) Limited change in dune mobility in response to a large decrease in wind power in semi-arid northern China since the 1970s. Geomorphology 102(3–4):351–363. https://doi.org/10.1016/j.geomorph.2008.04.004

Mcvicar TR, Van Niel TG, Li LT, Roderick M, Rayner DP, Ricciardulli L, Randall JD (2008) Wind speed climatology and trends for Australia, 1975–2006: capturing the stilling phenomenon and comparison with near-surface reanalysis output. Geophys Res Lett 35(20):288–299. https://doi.org/10.1029/2008GL035627

Paredes P, Fontes JC, Azevedo EB, Pereira LS (2017) Daily reference crop evapotranspiration with reduced data sets in the humid environments of Azores islands using estimates of actual vapor pressure, solar radiation, and wind speed. Theor Appl Climatol 134:1–19. https://doi.org/10.1007/s00704-017-2329-9

Pirazzoli PA, Tomasin A (2003) Recent near-surface wind changes in the Central Mediterranean and Adriatic areas. Int J Climatol 23:963–973. https://doi.org/10.1002/joc.925

Pryor SC, Barthelemie RJ, Schoof JT (2005) Inter annual variability of wind indices across Europe. Wind Energy 9:27–38. https://doi.org/10.1002/we.178

Pryor SC, Barthelmie RJ, Young DT, Takle ES, Arritt RW, Flory D, Gutowski WJ, Nunes A, Roads J (2009) Wind speed trends over the contiguous United States. J Geophys Res Atmos 114(D14). https://doi.org/10.1029/2008JD011416

Pu ZC, Zhang SQ, Li JL, Wang SL, Liu HR, Li J (2010) Climate change of area around Taklimakan Desert during 1961—2007. J Desert Res 2:413–422. https://doi.org/10.3788/HPLPB20102207.1462

Rittner M, Vermeesch P, Carter A, Bird A, Stevens T, Garzanti E, Andò S, Vezzoli G, Dutt R, Xu ZW, Lu HY (2016) The provenance of Taklamakan desert sand. Earth Planet Sci Lett 437:127–137. https://doi.org/10.1016/j.eps;.2015.12.036

Smits A, Klein-Tank AMG, Können GP (2005) Trends in storminess over the Netherlands, 1962–2002. J Desert 25(10):1331–1344. https://doi.org/10.1002/joc.1195

Tian L (2012) Studies on characteristics and impact factors of the surface wind speed changes in the northern China. LanZhou University, Lanzhou

Vautard R, Cattiaux J, Yiou P, Thépaut JN, Ciais P (2010) Northern hemisphere atmospheric stilling partly attributed to an increase in surface roughness. Nat Geosci 3(11):756–761. https://doi.org/10.1038/ngeo979

Von-Axe WS (1975) Energy: natural limits and abundance. EOS Trans Amer Geophys Union 55:828–832. https://doi.org/10.1029/EO055i009p00828

Wang HJ (2001) The weakening of the Asian monsoon circulation after the end of 1970's. Adv Atmos Sci 18(3):376–386. https://doi.org/10.1007/BF02919316

Wang XM, Dong ZB, Zhang JW, Chen GT (2002) Geomorphology of sand dunes in the Northeast Taklimakan Desert. Geomorphology, 42(3-4):183-195. https://doi.org/10.1016/S0169-555X(01)00085-X

Wang XM, Li JJ, Dong GR, Xia DS (2007) Nearly 50 years came to the wind and sand climate change and desertification response in the sand area of northern China. Chin Sci Bull 52(24):2882–2888. https://doi.org/10.3321/j.issn:0023-074x.2007.24.011

Wu Z (1981) Approach to the genesis of the Taklamakan Desert. Acta Geograph Sin 36(3):280–291

Xiao N, Dong ZB, Nan WG, Cui XJ, Li C, Xiao WQ, Li LL (2018) Characteristics of surface wind field in the Hobq Desert from 1957 to 2014. J Desert Res 38(3):1–9. https://doi.org/10.7522/J.ISSN.1000-694x.2017.00034

Xu M, Chang C, Fu C, Qi Y, Robock A, Robinson D, Zhang HM (2006) Steady decline of east asian monsoon winds, 1969–2000: evidence from direct ground measurements of wind speed. J Geophys Res Atmos 111(D24). https://doi.org/10.1029/2006JD007337

Xu Y, Yang J, Chen Y (2016) NDVI-based vegetation responses to climate change in an arid area of China. Theor Appl Climatol 126(1–2):213–222. https://doi.org/10.1007/s00704-015-1572-1

Yang XP (1992) Geomorphologische Untersuchungen in trockenraeumen NW-Chinas unter besonderer Beruecksichtigung von Badanjilin und Takelamagan. Goettinger Geographische Abhandlungen 96:1–36

Yang YH, Zhao N, Hao XH, Li CQ (2009) Decreasing trend in sunshine hours and related driving force in North China. Theor Appl Climatol 97(1):91–98. https://doi.org/10.1007/s00704-008-0049

Yang XP, Li HW, Conacher A (2012) Large-scale controls on the development of sand seas in northern China. Quat Int 250:74–83. https://doi.org/10.1016/j.quaint.2011.03.052

Young IR, Zieger S, Babanin AV (2011) Global trends in wind speed and wave height. Science 332(6028):451–455. https://doi.org/10.1126/science.1197219

Zhang DH (1984) A preliminary analysis to the dust climatology of China from historical period. Chin Sci 3:278–288

Zhang ZC, Dong ZB (2014) Dune field patterns and wind environments in the middle reaches of the Heihe Basin. J Desert Res 34(2):332–341. https://doi.org/10.7522/j.issn.1000-694X.2013.00323

Zhang YQ, Liu CM, Tang YH, Yang YH (2007) Trends in pan evaporation and reference and actual evapotranspiration across the Tibetan plateau. J Geophys Res Atmos 112(D12). https://doi.org/10.1029/2006jd008161

Zhang ZC, Dong ZB, Zhao AG, Qiang GQ (2010) Characteristics of blown sand activity in the Kumtagh Desert. Arid Land Geogr 33(6):939–946. https://doi.org/10.1017/S0004972710001772

Zhang KC, Ao YH, Qu JJ, An ZS (2013) Dynamical environments of wind-blown sand near lakes surrounded by sand-mountains in the Badain Jaran Desert. Arid Land Geogr 36(5):790–794. https://doi.org/10.13826/j.cnki.cn65-1103/x.2013.05.005

Zhao CY, Si JH, Feng Q, Yu TF, Li PD (2015) Effect of wind speed on transpiration rate of Populus euphratica in extreme arid deserts. J Glaciol Geocryol 37(4):1104–1111

Zheng J, Li B, Chen Y, Che L (2017) Spatiotemporal variation of upper-air and surface wind speed and its influencing factors in northwestern china during 1980–2012. Theor Appl Climatol:1–12. https://doi.org/10.1007/s00704-017-2346-8

Zhu ZD, Chen Z, Wu Z, Li B, Wu G (1981) Study on the geomorphology of wind-drift sands in the Taklimakan Desert. Science Press, Beijing

Zu RP, Zhang KC, Qu JJ, Fang HY (2005) Study on wind regime characteristics in the Taklimakan Desert. Arid Land Geogr 28(2):167–170. https://doi.org/10.13826/j.cnki.cn65-1103/x.2005.02.006

Zu R, Xue X, Qiang M, Yang B, Qu J, Zhang K (2008) Characteristics of near-surface wind regimes in the Taklimakan desert, China. Geomorphology 96(1):39–47. https://doi.org/10.1016/j.geomorph.2007.07.008